J Neuropathol Exp Neurol
Vol. 72, No. 11
November 2013
pp. 1062–1071

ORIGINAL ARTICLE

OPEN

A Rapid Gene Delivery–Based Mouse Model for Early-Stage Alzheimer Disease–Type Tauopathy

Robert Siman, PhD, Yin-Guo Lin, MS, Gauri Malthankar-Phatak, PhD, and Yina Dong, PhD

Abstract

The perforant pathway projection from the entorhinal cortex (EC) to the hippocampal dentate gyrus is critically important for long-term memory and develops tau and amyloid pathologies and progressive degeneration starting in the early stages of Alzheimer disease (AD). However, perforant pathway function has not been assessed in experimental models of AD, and a therapeutic agent that protects its structure and function has not yet been identified. Therefore, we developed a new adeno-associated virus–based mouse model for perforant pathway tauopathy. Microinjection into the lateral EC of vectors designed to express either human tau bearing a pathogenic P301L mutation or enhanced green fluorescent protein as a control selectively drove transgene expression in lateral EC layer II perikarya and along the entire rostrocaudal extent of the lateral perforant pathway afferents and dentate terminal field. After human tau expression, hyperphosphorylated tau accumulated only within EC layer II perikarya, thereby modeling Braak stage I of transentorhinal AD tauopathy. Expression of pathologic human tau but not enhanced green fluorescent protein led to specific dose-dependent apoptotic death of perforant pathway neurons and loss of synapses in as little as 2 weeks. This novel adeno-associated virus–based method elicits rapid tauopathy and tau-mediated neurodegeneration localized to the mouse perforant pathway and represents a new experimental approach for studying tau-driven pathogenic processes and tau-based treatment strategies in a highly vulnerable neural circuit.

Key Words: Adeno-associated virus, Apoptosis, Early-stage Alzheimer disease, Entorhinal cortex, Hippocampus, Perforant pathway, Tauopathy.

From the Department of Neurosurgery and Center for Brain Injury and Repair, University of Pennsylvania School of Medicine, Philadelphia, Pennsylvania.

Send correspondence and reprint requests to: Robert Siman, PhD, Department of Neurosurgery, Perelman School of Medicine, University of Pennsylvania, 502 Stemmler Hall, 36th and Hamilton Walk, Philadelphia, PA 19104; E-mail: siman@mail.med.upenn.edu

This work was supported by an Alzheimer's Association Zenith Award to Robert Siman and a Penn Institute on Aging Pilot grant to RS (parent award AG010124 to Dr. John Trojanowski).

Supplemental digital content is available for this article. Direct URL citations appear in the printed text and are provided in the HTML and PDF versions of this article on the journal's Web site (www.jneuropath.com).

INTRODUCTION

There is considerable evidence that dysfunction of the perforant pathway projection from the entorhinal cortex (EC) to the hippocampal dentate gyrus is an important contributor to the onset and progression of cognitive impairment in Alzheimer disease (AD). This pathway is a major source for excitatory innervation of the hippocampus, a structure vital for memory formation (1,2). Damage to the EC in rats causes a rapid forgetting syndrome reminiscent of that occurring in AD patients (3). The perforant pathway is particularly vulnerable in AD. The entorhinal neurons of origin in layer II are among the first to develop aggregates of the microtubule-associated protein tau in the form of neurofibrillary tangles (Braak stage I), characterized by superficial entorhinal tauopathy (4), and the terminal field in the dentate gyrus is a preferential early site for β-amyloid deposition (5). Recent evidence suggests that tauopathy initiating in the perforant pathway spreads over time through its afferent connections (6, 7). Moreover, the pathway exhibits neurodegeneration beginning with the earliest signs of cognitive impairment; and the neuronal loss progresses coincident with cognitive decline, until more than 90% of the pathway has degenerated (8–10). Consequently, studying the molecular mechanisms leading to progressive perforant pathway tauopathy, dysfunction and degeneration should provide insights into AD pathogenesis.

Alzheimer disease is one of several neurodegenerative tauopathies for which tau aggregation into oligomers, paired helical filaments, and neurofibrillary tangles have been linked to disease pathogenesis (11, 12). An important feature is tau hyperphosphorylation, which reduces its association with microtubules and promotes its propensity for aggregation. A number of tau-based therapeutic approaches for AD directed at stabilizing microtubules, physically blocking tau aggregation, inhibiting protein kinases involved in tau hyperphosphorylation, and removing extracellular tau immunologically are being explored, but there are few functional studies of tauopathy-induced neural circuit dysfunction, and a tau-based therapeutic agent that preserves the synaptic function of vulnerable neural circuits important for cognition, such as the perforant pathway, has not yet been identified.

Mouse lines expressing mutant tau transgenes that in humans cause the inherited tauopathy frontotemporal lobar degeneration (FTD) reproduce some histopathologic and behavioral features of the progressive tauopathy of AD (13–18). Unfortunately, the models develop tau pathology in cell populations such as spinal motor, basal ganglia, and dentate granule neurons that are not preferentially impacted in AD but contribute

to the observed behavioral phenotypes. Moreover, cognitive performance in the mouse is a complex and indirect measure of dysfunction in specific neural circuits, and it is a difficult stand-alone end point for the preclinical study of molecular and cellular pathogenic mechanisms of AD or development and optimization of therapeutic candidates directed at progressive tauopathy. Furthermore, despite numerous studies of pathologic tau-dependent neurodegeneration in cultured cell and transgenic models, there is no consensus on the mechanism(s) of tau-driven neurotoxicity (19–25). As an alternative to transgenic and cell culture approaches, adeno-associated virus 2 (AAV2) vector–based delivery of pathologic human tau to the rat entorhinal cortex has been described, but human tau expression is absent from the perforant pathway terminal field and spatially limited within the entorhinal cortex (26). As a versatile model for early-stage AD tauopathy, we describe the development and initial characterization of a novel AAV-based gene delivery method that induces human tau expression and tau-driven pathology focally and rapidly in the mouse perforant pathway.

MATERIALS AND METHODS

AAV Vectors

A cDNA encoding full-length 441–amino acid human 4 repeat tau bearing a P301L mutation was generously provided by Dr. Virginia Lee. All of the AAV vectors were cloned, produced in scale, purified, and sequence verified by the Penn Vector Core Facility in the Department of Genetics under the direction of Dr. Julie Johnson. The virus particle concentrations were calculated as the number of viral genome copies per unit volume.

Stereotaxic Neurosurgical Methods for Delivering AAV Vectors to Mouse Brain

The AAV vectors were microinjected unilaterally to the right lateral entorhinal area by stereotaxic convection–enhanced delivery (27). The protocol was reviewed and approved by the Penn Institutional Animal Care and Use Committee. Male CD-1 mice, 3 to 4 months old and weighing approximately 35 g, were anesthetized with ketamine/xylazine/acepromazine, and the surgery was performed under aseptic conditions. Stereotaxic coordinates were (from bregma) anteroposterior, −4.0 mm; lateral, 4.5 mm; vertical, 2.9 mm from the pial surface. A 27-gauge cannula was fitted with a silica microtube insert (Polymicro Technologies, Phoenix, AZ) affixed with superglue and attached to a Hamilton syringe for delivery of AAV vectors in 0.5 μL sterile saline at doses ranging from 0.5 to 5×10^9 virus particles. The volume was injected for a 5-minute period, and the cannula was left in place for an additional 3 minutes before slowly being raised over another 3-minute period. Postsurgical pain relief was provided by presurgical administration of buprenorphine and postsurgical injection of meloxicam. A total of 34 mice were evaluated after receiving 3×10^9 AAV2/9-hTauP301L virus particles in the study: 18 at 3 weeks postinjection (pi), 9 at 6 weeks pi, and 7 at 10 to 14 weeks pi. A total of 32 mice were studied after receiving 1.5×10^9 virus particles: 20 at 2 to 3 weeks pi and 12 at 12 to 14 weeks pi. A total of 24 mice were evaluated after receiving 0.5×10^9 virus particles: 11 at 3 weeks and 13 at 12 to 14 weeks pi. An additional 13 mice were injected with 3×10^9 AAV2/9–enhanced green fluorescent protein (eGFP) virus particles: 8 were analyzed at 3 weeks pi and 5 at 9 to 12 weeks pi.

Mice were given free access to food and water and maintained under veterinary supervision in strict compliance with all standards for animal care and investigation established in the *Guide for the Care and Use of Laboratory Animals* (National Academy Press ISBN 0-309-05377-3).

Immunohistochemical, Immunofluorescence, Morphometric, and Histochemical Methods

At pi times ranging from 9 to 100 days, mice were deeply anesthetized with an overdose of pentobarbital and perfused transcardially with ice-cold sodium phosphate buffer ([PB] 0.1 mol/L, pH 7.4), followed by freshly prepared and filtered 4% paraformaldehyde in PB. Brains were postfixed for 4 to 5 hours, cryoprotected in 20% sucrose in PB overnight, blocked for sectioning in the coronal plane, frozen at −40°C, and stored at −80°C. Coronal 40-μm sections were prepared on a sliding microtome and collected into 10 series, starting at the posterior cortex and extending anteriorly through the hippocampus. Immunohistochemical staining was performed by published avidin-biotin-immunoperoxidase methods (28, 29) using the following mouse monoclonal antibodies to tau (purchased from ThermoFisher, Rockford, IL): biotinylated HT7 (1:1000; specific for human but not mouse tau), biotinylated AT8 (1:1000; specific for tau phosphorylated on Ser202/Ser205), biotinylated PHF6 (1:1000; specific for tau phosphorylated on Thr231), and biotinylated AT100 (1:800; specific for tau phosphorylated on Thr212/Ser214/Ser217). The PHF1 antibody reactive with tau phosphorylated on Ser396/Ser404 was generously provided as a hybridoma supernatant by Dr. Peter Davies and used at 1:50. The biotinylated primary antibodies improved the specificity of mouse brain immunostaining by obviating the need for an anti-mouse IgG secondary antibody that cross-reacts with mouse immunoglobulins expressed on the surface of microglial cells. Twelve of the mice received simultaneous coinjections with the tau and eGFP vectors for analyzing colocalization of the expressed proteins by immunofluorescence/fluorescence.

For quantitative morphometric analysis of neuronal survival, 2 series of sections from each brain were immunostained for the neuronal nuclear marker NeuN using a biotinylated mouse monoclonal antibody at 1:5000 (Abcam, Cambridge, MA). For each section, the density of NeuN-positive neuronal nuclei in layer II was compared between the injected and uninjected lateral entorhinal areas using Nikon NIS Elements software. A region of interest encompassing layer II was defined in the lateral EC starting at the border between the piriform and entorhinal cortex beneath the rhinal fissure and extending ventrally 0.8 to 1 mm, depending on the rostrocaudal plane, to the intermediate entorhinal area. Photomicrographs of anti-NeuN–stained EC were processed by binary thresholding. For each section, neuronal survival in layer II of the injected lateral EC was defined as the percent of the region of interest occupied by NeuN staining in relation to the contralateral region at an equivalent rostrocaudal plane. For each mouse, 2 sections at levels caudal to the AAV microinjection site and another 2 at levels rostral to the injection site were analyzed, covering a

rostrocaudal area extending 1.6 mm (30). For each treatment group, from 4 to 11 mice were evaluated for lateral entorhinal layer II neuronal survival.

Caspase substrate proteolysis was analyzed by immunostaining with Ab246, a rabbit antibody specific for the caspase cleavage motif PRDETD found at the COOH-terminus of a caspase-derived α-spectrin fragment, along with other caspase substrates (31, 32). For immunoperoxidase staining, Ab246 was used at 1:10,000; whereas for immunofluorescence, the antibody was diluted 1:1500. Neuronal nuclei were identified by colabeling for NeuN with the biotinylated mouse antibody at 1:500 dilution and human tau expressing neurons by colabeling for HT7 using the biotinylated mouse antibody at 1:200. The double immunofluorescence method used as secondary probes goat anti-rabbit IgG–Alexa Fluor 568 and streptavidin–Alexa Fluor 488 (Life Technologies, Grand Island, NY), both diluted to 1:750. Nuclei were counterstained with Hoechst 33342 and visualized under UV illumination. Nuclear morphologies were examined at 400× magnification by capturing a series of z-stack images and processing them for digital sectioning by image deconvolution microscopy.

Histochemical staining for zinc was performed using the Timm silver sulfide method (33). Fluorescent labeling of acutely degenerating cells was performed using Fluoro-Jade B (34). The Gallyas silver method was used to label neurofibrillary pathology (35).

RESULTS

Identification of an AAV Vector That Drives Focal Gene Expression in the Mouse Perforant Pathway

Several AAV vectors of varying serotypes, gene promoters, and regulatory elements were evaluated for transduction of the mouse perforant pathway initially using an eGFP reporter transgene. Based on preliminary findings, we focused on AAV2/1 and 2/9 serotypes and the synapsin I gene promoter. All 3 of the eGFP vectors shown schematically in Figure 1 generated reporter expression exclusively in neurons and to varying magnitudes after stereotaxic convection-enhanced delivery into the lateral entorhinal area (27). Based on reports that the woodchuck hepatitis virus posttranscriptional regulatory element (WPRE) can markedly stabilize viral vector–encoded mRNA (36) and enhance transgene expression in a neuronal cell type–dependent manner (37, 38), we examined its effect on entorhinal transgene expression in the context of the AAV9 serotype and synapsin I promoter. The WPRE dramatically increased eGFP expression confined to the layer II neurons of origin for the mouse perforant pathway. By 3 weeks pi of 3×10^9 or fewer virus particles, eGFP expression was restricted to a band of lateral entorhinal neuronal perikarya in layer II ventral to the rhinal fissure (Fig. 2A, B), to the dendrites of these neurons, to perforant pathway afferents (39) in the hippocampal

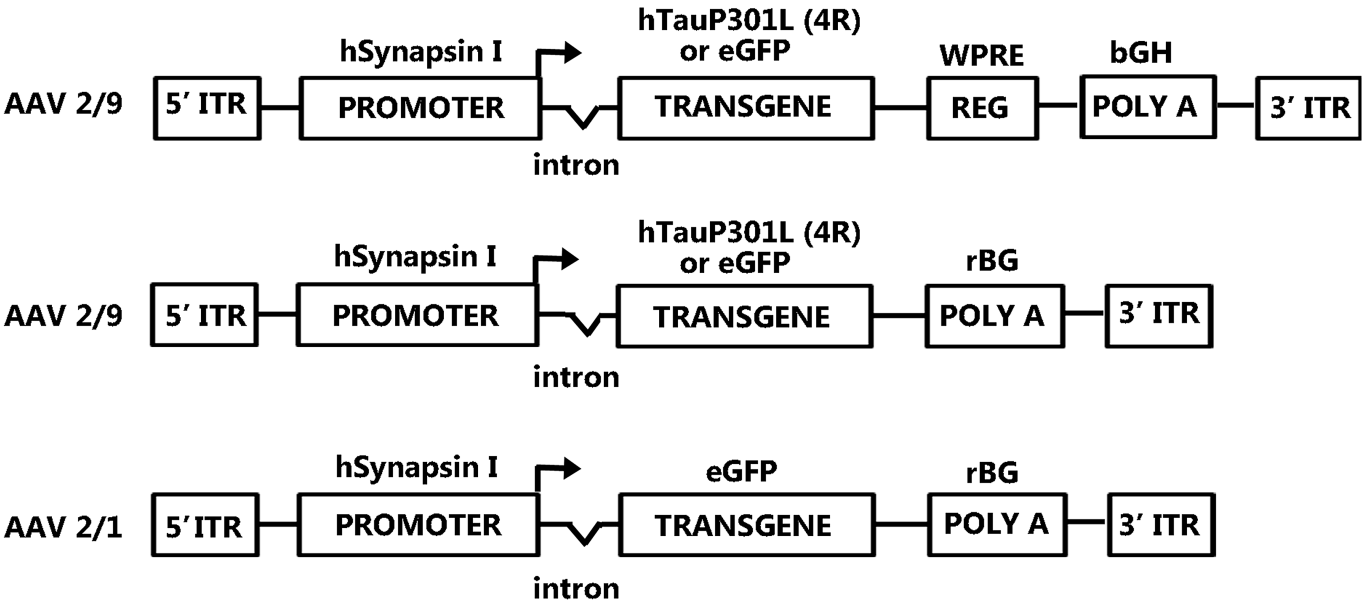

FIGURE 1. Schematic diagram of the AAV vectors and serotypes tested for driving perforant pathway gene expression. The vectors use the human synapsin I promoter to drive neuron-specific gene expression and AAV serotypes 2/9 and 2/1 to direct efficient transduction of adult brain neurons and encode either human tau bearing a frontotemporal degeneration-linked P301L mutation or eGFP. The best results for inducing long-lasting, strong, and focal transgene expression in the mouse perforant pathway are obtained by incorporating the WPRE 3′ to the transgene. bGH, bovine growth hormone; eGFP, enhanced green fluorescent protein; ITR, inverted terminal repeat; rBG, rabbit β-globin regulatory element; REG, regulatory sequence; WPRE, woodchuck hepatitis virus posttranscriptional regulatory element.

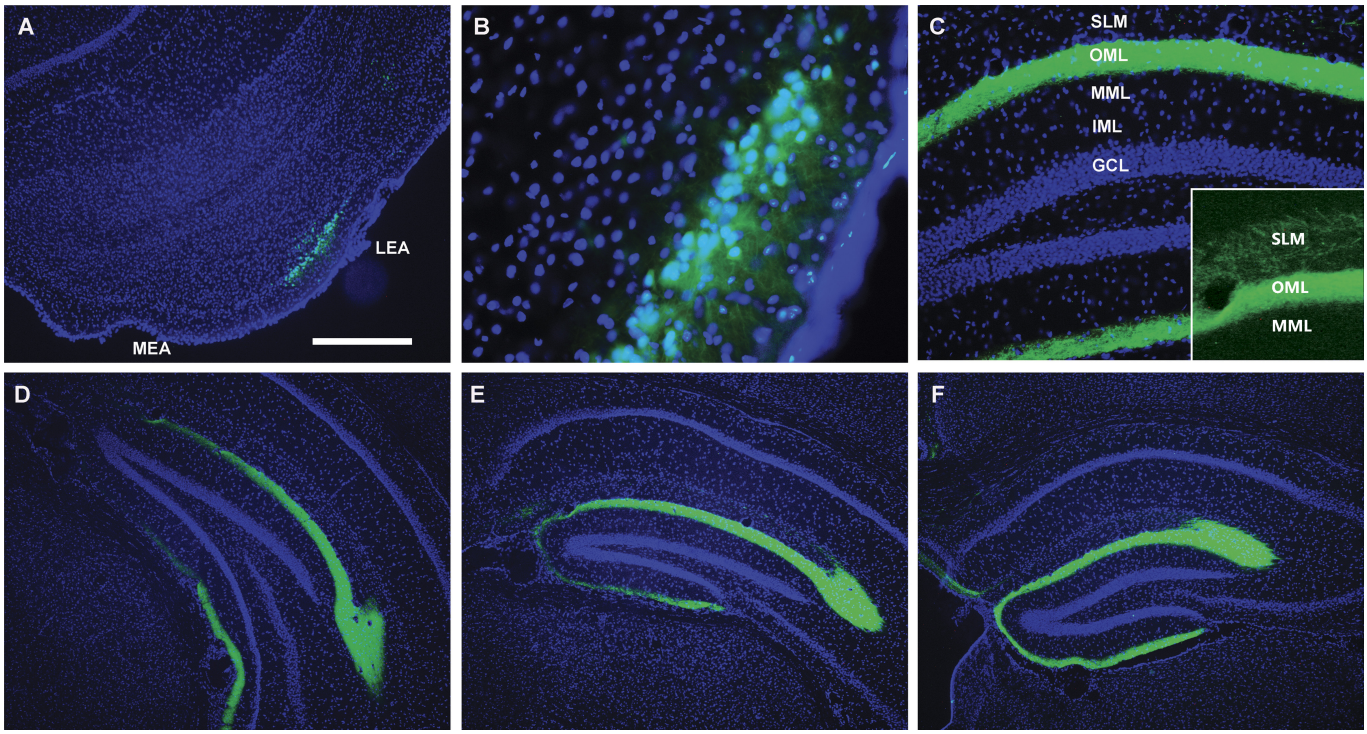

FIGURE 2. Identification of an AAV vector that drives gene expression focally throughout the mouse perforant pathway. At 3 weeks after intraentorhinal microinjection of 1×10^9 particles of AAV2/9–synapsin I promoter–eGFP–WPRE, enhanced green fluorescent protein (eGFP) is expressed predominantly in entorhinal cortex (EC) layer II neurons and along the entire rostrocaudal extent of the lateral perforant pathway projection. Low-power (**A**) and high-power (**B**) photomicrographs taken immediately rostral to the injection site in the lateral entorhinal area (LEA) visualizing eGFP in green and counterstained nuclei in blue. Enhanced GFP expression is confined to layer II of the LEA and the dendritic processes of these neurons but is absent from the medial entorhinal area (MEA) and cells in other layers of entorhinal cortex. (**C**) In the hippocampus, 3 weeks after intraentorhinal vector delivery, eGFP expression is present in the perforant pathway afferents traversing the hippocampal stratum lacunosum-moleculare (SLM, inset) and strong in the terminal field for the lateral perforant pathway in the dentate gyrus outer molecular layer (OML) but is absent from the middle and inner molecular layers (MML and IML), respectively, the granule cell layer (GCL), and the adjacent regions of the hippocampus. Enhanced GFP expression in the lateral perforant pathway terminal field is strong at caudal (**D**), intermediate (**E**), and rostral (**F**) levels of the hippocampal formation. Scale bars = **(A)** 400 μm; **(B, C)** 150 μm; **(D–F)** 250 μm.

stratum lacunosum-moleculare (Fig. 2C inset), and to the lateral perforant pathway terminal field in the dentate gyrus outer molecular layer (OML) (Fig. 2C). Transgene expression was strong along the entire rostrocaudal extent of the synaptic field of the lateral perforant pathway (Fig. 2D–F).

Expression of Pathologic Human Tau in the Mouse Lateral Perforant Pathway: A Model for Early-Stage Entorhinal AD-Type Tauopathy

Based on the results with eGFP expression, we constructed an AAV2/9–synapsin I promoter–Tau–WPRE vector to drive human tau expression in the mouse perforant pathway. The vector encodes full-length 441–amino acid human tau bearing 4 repeats and an FTD-linked pathogenic P301L mutation, a form that in transgenic mouse lines elicits slowly progressive tau pathology in many regions of the CNS (13–15). Immunohistochemical staining for tau using the human specific phospho-independent monoclonal HT7 revealed robust transgene expression at 3 weeks pi in the lateral entorhinal area, the hippocampus proper, and the dentate gyrus (Fig. 3A). Human tau was localized in the EC layer II neurons of origin and their dendritic processes (Fig. 3C, D) and followed the known trajectory of the mouse perforant pathway projection (39), entering the hippocampus in stratum lacunosum-moleculare (Fig. 3E, F), and perforating the hippocampal fissure to terminate in the OML of the dentate gyrus. Other synaptic fields in the hippocampus were devoid of human tau expression 3 weeks after AAV2/9–synapsin I–TauP301L–WPRE microinjection, and no other cell population or brain region contained human tau at this time point after well-placed vector microinjections were confined to the entorhinal cortex.

In as little as 3 weeks, intraentorhinal delivery of the tau vector induced the expression of a variety of phospho-tau epitopes restricted to the EC layer II neurons of origin for the lateral perforant pathway. The AT8 antibody, which is specific for tau phosphorylated on serine 202 and 205, labeled the lateral entorhinal cortex layer II neuronal perikarya and proximal processes (Fig. 3B, G), as did the PHF6 antibody, which recognizes tau phosphorylated on threonine 231 (Fig. 3H). In both instances, the perforant pathway afferents and dentate gyrus terminal field were devoid of phospho-tau immunolabeling, despite the presence of human tau in these regions detectable with HT7. The mouse brain at 3 to 6 weeks pi did not label with the PHF1 antibody specific for tau phosphorylated on residues 396 and 404 (data not shown). Neurofibrillary tangles stained by the

Gallyas silver method or the AT100 antibody specific for a late phospho-form of tau (40) appeared in the entorhinal cortex only starting at 6 weeks pi (Figure, Supplemental Digital Content 1, http://links.lww.com/NEN/A524). The expression of multiple tau phosphoforms restricted to entorhinal cortex layer II resembles the preferential localization of hyperphosphorylated and aggregated tau to the superficial EC neurons of origin for the perforant pathway at the Braak stage I of Alzheimer tauopathy (4, 41).

Human Pathologic Tau Causes Rapid Dose-Dependent Apoptosis of Mouse Entorhinal Neurons and Loss of Perforant Pathway Synapses

The perforant pathway is especially vulnerable to degeneration in AD: there is approximately 50% loss of EC layer II neurons in elderly individuals with mild cognitive impairment (8, 9, 42), and the pathway continues to degenerate concomitant with cognitive decline until more than 90% of the neurons have died (10). To investigate whether pathologic human tau is toxic for the mouse perforant pathway, we stained for the neuronal nuclear marker NeuN 3 weeks after AAV-driven expression of either tauP301L or eGFP. Compared with the uninjected contralateral EC (Fig. 4B), the expression of pathologic human tau induced pronounced loss of NeuN-positive neurons in the ipsilateral lateral EC layer II (Fig. 4A, arrowheads), coinciding with the circumscribed expression of human tau in these neurons. In contrast to the toxicity of tau, neither a comparable nor a higher dose of the eGFP vector was toxic (beyond a very minor amount of surgical trauma directly at the microinjection site) (Fig. 4C, F) and despite robust eGFP expression in lateral EC layer II neurons and the perforant pathway projection (Fig. 2). The toxicity of TauP301L for the lateral perforant pathway was dose dependent, producing up to an 81% loss of NeuN-positive lateral EC neurons (Fig. 4F). Nevertheless, human tau expression was readily detectable even at a dose of 0.5×10^9 virus particles that was not acutely toxic. The reduction in surviving NeuN-positive neurons at higher doses of the tau vector was not simply a loss of the NeuN marker because traditional histochemical methods also showed disappearance of layer II cells in the lateral EC ipsilateral to the vector injection (data not shown; see also below). No other brain area showed overt neuronal loss after intraentorhinal transduction of human tau.

Pathologic human tau triggered a rapid loss not only of the neurons of origin for the perforant pathway but also of

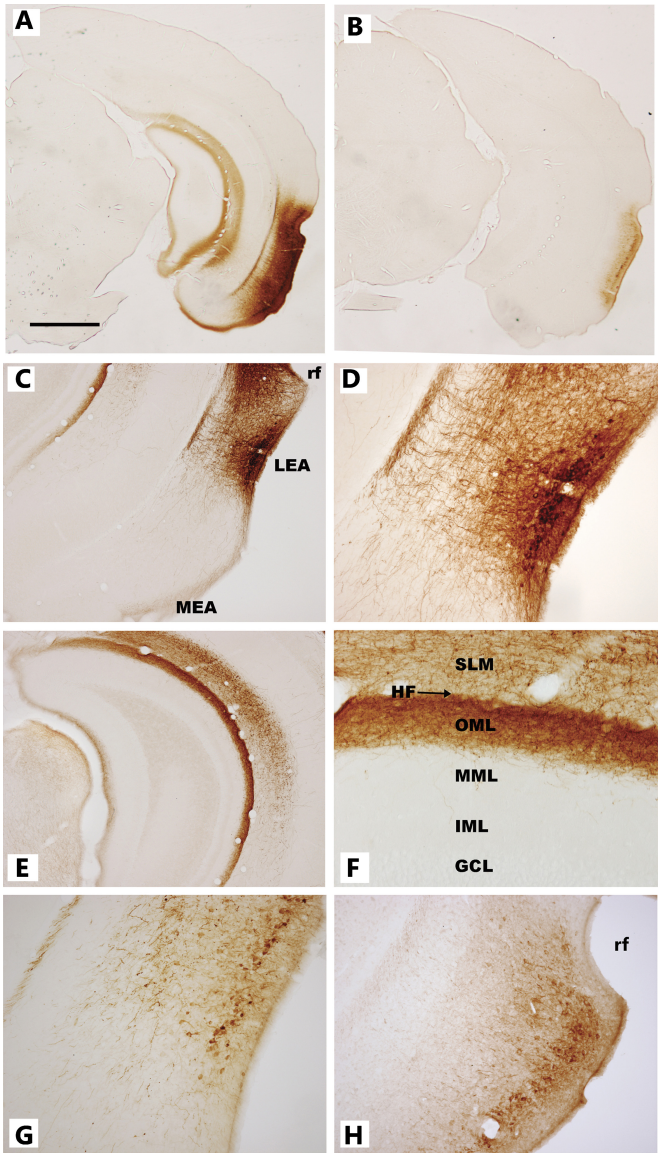

FIGURE 3. Pathologic human tau in the mouse perforant pathway mimics Braak stage I of Alzheimer tauopathy. This figure depicts human tau expression, hyperphosphorylation, and localization in the mouse lateral perforant pathway 3 weeks after intraentorhinal microinjection of 1.5×10^9 virus particles of AAV2/9–synapsin I promoter–hTauP301L–WPRE. **(A)** Low-power view of human tau expression in the injected hemisphere using the phosphorylation-independent HT7 monoclonal antibody specific for human but not mouse tau. Human tau expression after entorhinal microinjection of this dose of virus particles is confined to the lateral entorhinal area and hippocampal formation ipsilateral to the microinjection. **(B)** Low-power view of human phospho-tau202/205 labeled with antibody AT8. Unlike total human tau, phospho-tau202/205 is restricted to layer II neurons of the lateral entorhinal area. **(C, D)** Higher-power views of human tau in the entorhinal cortex stained with antibody HT7 illustrate that the tau transgene is expressed in the layer II neurons of origin for the lateral perforant pathway in the lateral entorhinal area (LEA), their dendritic processes, and the axons of the perforant pathway. **(E, F)** Higher-power views of human tau in the hippocampal formation stained with HT7. The human tau is expressed in the perforant pathway projection in stratum lacunosum-moleculare of the hippocampal CA1 sector (SLM) and the lateral perforant pathway terminal field in the outer molecular layer (OML) of the dentate gyrus adjacent to the hippocampal fissure (HF). In contrast, the dentate middle and inner molecular layers (MML and IML, respectively) and granule cell layer (GCL) are devoid of human tau. **(G, H)** Higher-power photomicrographs of hyperphosphorylated tau concentrated in the lateral perforant pathway neurons of origin in layer II of the lateral entorhinal area: **(G)** pTau202/205; **(H)** pTau231. Scale bars = **(A, B)** 1 mm; **(C, E)** 400 μm; **(D, G, H)** 160 μm; **(F)** 80 μm.

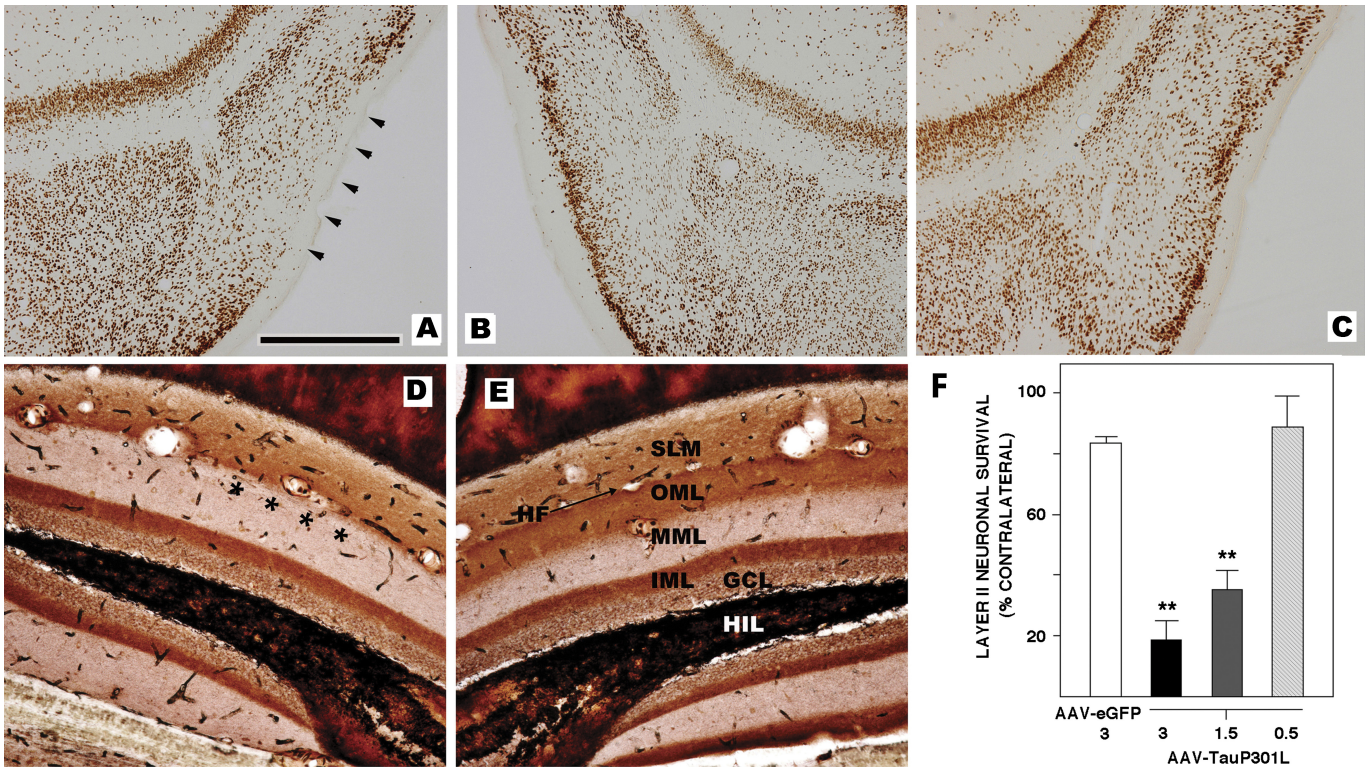

FIGURE 4. Pathologic human tau rapidly induces perforant pathway degeneration and synapse loss. In as little as 3 weeks after unilateral entorhinal delivery of 1.5 to 3 $\times$ 10^9 particles of the human tau vector, immunostaining for the neuronal nuclear marker NeuN reveals profound loss of layer II neurons in the lateral entorhinal area. (**A**) Ipsilateral entorhinal cortex (EC), 1.5 $\times$ 10^9 virus particles; arrowheads denote the layer II neuronal loss. (**B**) Contralateral EC. (**C**) In contrast, there is little change in the number of NeuN-positive neurons in the ipsilateral EC 3 weeks after intraentorhinal delivery of 3 $\times$ 10^9 particles of the enhanced green fluorescent protein (eGFP) vector. (**D, E**) Loss of lateral perforant pathway synapses 6 weeks after intraentorhinal delivery of the pathologic human tau. Timm staining reveals the normal pattern of afferent lamination of the dentate gyrus and the zones of relatively high zinc content in the lateral perforant pathway terminal field in the outer molecular layer (OML) of the dorsal and ventral blades contralateral to the AAV microinjection (**E**). In the ipsilateral hippocampal formation, there is pronounced loss of the OML; zones of zinc staining in both blades of the dentate gyrus indicate terminal degeneration (**D**, asterisks; compare with **E**). (**F**) Quantitative analysis of the dose-dependent toxicity of pathologic human tau for mouse lateral perforant pathway neurons. After injections of 3 $\times$ 10^9 eGFP virus particles or 0.5 $\times$ 10^9 tau virus particles, neuronal survival was not significantly different compared with that of the uninjected hemisphere. Higher doses of the tau vector caused significant perforant pathway neuronal loss (** $p < 0.002$ vs eGFP control). Scale bars = **(A–C)** 500 μm; **(D, E)** 250 μm.

perforant pathway synapses. Labeling of the dentate gyrus with the nerve terminal marker synaptophysin showed that, at 6 weeks after pathologic human tau expression, the synaptic density was reduced in the lateral perforant pathway terminal field in the OML and the molecular layer shrank (Figure, Supplemental Digital Content 2, http://links.lww.com/NEN/A525); this is an established response to perforant pathway partial deafferentation (43–45). It should be noted that widely expressed nerve terminal markers underestimate or fail entirely to show losses of lateral perforant pathway synapses because damage to this pathway triggers sprouting of medial perforant pathway afferents and reactive synaptogenesis in the denervated OML (43, 46). For an alternative pathway-specific approach, the lateral and medial perforant pathway terminal fields are distinguishable from one another and from neighboring synaptic zones by their differential content of zinc, which is concentrated within synaptic vesicles and can be visualized with Timm staining (47, 48). As shown in Figure 4E, the uninjected contralateral dentate gyrus contains bands of zinc staining in the OML of both the dorsal and ventral blades that differ in intensity from the adjacent middle molecular layer, containing the medial perforant pathway terminal field, as well as from the stratum lacunosum-moleculare in the hippocampal CA1 sector. At 6 weeks after delivery of a dose of the human tauP301L vector that causes extensive degeneration of layer II neurons in the lateral EC, there was near complete loss of the zinc-rich lateral perforant pathway nerve terminals in the OML of both blades of the dentate gyrus (Fig. 4D vs E).

To begin to examine the mechanism by which pathologic human tau is toxic for the mouse perforant pathway, we performed a time course experiment using Fluoro-Jade B staining to identify acutely degenerating neurons (25). As depicted in Figure 5, a large number of cells localized exclusively to the lateral EC layer II underwent degeneration from 12 to 14 days after delivery of the tau vector (Fig. 5A, B). At this time point, a subset of layer II neurons was immunopositive for a caspase-derived α-spectrin fragment (Fig. 5C, D), raising the possibility that pathologic tau may trigger caspase-mediated apoptosis.

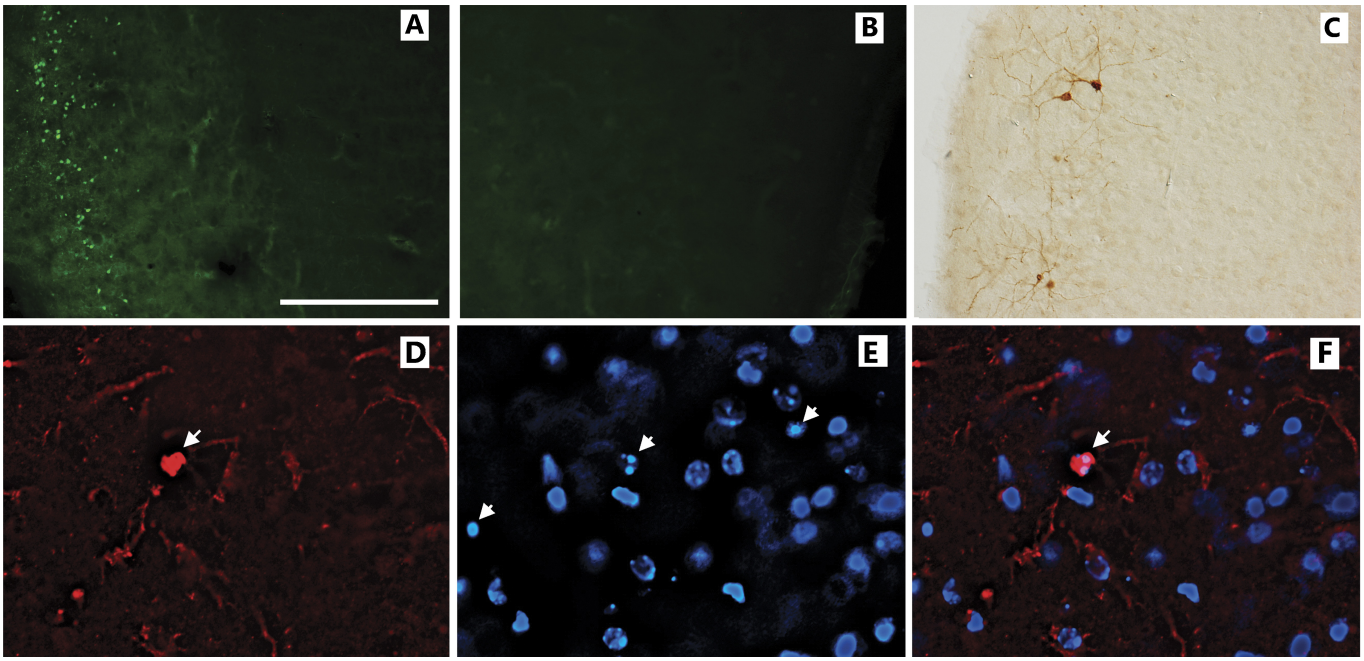

FIGURE 5. Evidence that the AAV-tau vector rapidly induces apoptosis of perforant pathway neurons. Expression of pathologic human tau at 14 days causes acute degeneration in the lateral entorhinal cortex (EC) visualized with Fluoro-Jade B ipsilateral (**A**) but not contralateral (**B**) to viral vector injection. In (**A**), note that human tau triggers degeneration confined to EC layer II. (**C**) Caspase substrate degradation in a subset of layer II neurons in the lateral EC 14 days after gene delivery (stained by an immunoperoxidase method with antibody Ab246 specific for a caspase cleavage motif). (**D**–**F**) Double fluorescence staining for chromatin and cleaved caspase substrates. Caspase substrate proteolysis in a neuron and its proximal dendritic processes in layer II of the lateral EC, Ab246 staining (**D**, arrow). Cells with condensed chromatin characteristic of an apoptotic nuclear morphology (**E**, arrows) in the same section stained with Hoechst 33342. (**F**) Merged images illustrate that a neuron positive for caspase-cleaved substrate also contains chromatin that is condensed and fragmented into apoptotic bodies (arrow). Scale bars = **(A, B)** 500 μm; **(C)** 200 μm; **(D**–**F)** 50 μm.

Inspection of nuclear morphologies after chromatin staining with Hoechst 33342 confirmed that some cells in the lateral EC layer II ipsilateral to the tau vector injection had condensed chromatin characteristic of apoptotic nuclear morphology (Fig. 5E, arrows). A subset of the cells with apoptotic nuclei colabeled for caspase-cleaved α-spectrin (Fig. 5F). In contrast, neither caspase proteolysis nor apoptotic nuclear morphologic profiles were observed in the contralateral EC or any other neocortical region. The induction of apoptosis by pathologic tau in perforant pathway neurons of origin was confirmed using triple labeling for human tau, caspase activation, and chromatin. Using triple labeling with 1-μm z-sectioning, a subset of the human tau expressing neurons in lateral EC layer II had simultaneously an abnormal ovoid and shrunken morphology (Fig. 6A, C), caspase-cleaved α-spectrin (Fig. 6B, C), and chromatin that was condensed and fragmented into apoptotic bodies (Fig. 6D, arrow).

Polysynaptic Spread of Human Tau From the Mouse Perforant Pathway

Recent evidence from in vitro and in vivo studies indicates that tau is released from neurons and taken up by neighboring ones and can transfer between synaptically interconnected neurons, where it may promote the spread of tauopathy via templated misfolding (6, 7, 49). To investigate whether human tau spreads from the entorhinal cortex via the lateral perforant pathway afferents in the AAV mouse model, we searched for human tau expression in the dorsal hippocampus various times after tau gene delivery to the lateral EC. At the 3-week time point, human tau in the dorsal hippocampal formation was confined to the perforant pathway projection in stratum lacunosum-moleculare and terminal field in OML (Figs. 3, 7). By 10 to 14 weeks, however, human tau expression expanded to include dentate granule neurons, which are the targets for the perforant pathway, the granule neuron axons and boutons comprising the mossy fiber pathway in stratum lucidum, and a small number of mossy fiber target neurons in stratum pyramidale in the CA3 region (Fig. 7). On the other hand, during a 14-week period, there was no evidence for spread of hyperphosphorylated tau, as tau phosphorylated on serine 202 and 205 or threonine 231 remained restricted to surviving neurons in the superficial EC (data not shown). Polysynaptic spread of protein to perforant pathway targets was not observed at comparable or even higher doses of the AAV-eGFP vector (data not shown).

DISCUSSION

Here we describe a viral vector–based method for expressing genes focally throughout the mouse perforant pathway using the AAV2/9 serotype, synapsin I gene promoter, and WPRE. Using this approach, expression of human tau bearing an FTD-linked P301L mutation elicits within weeks tau hyperphosphorylation and the perikaryal accumulation of hyperphospho-tau in lateral entorhinal cortex layer II, along with tau-mediated degeneration of lateral perforant pathway neurons and synapses. The AAV

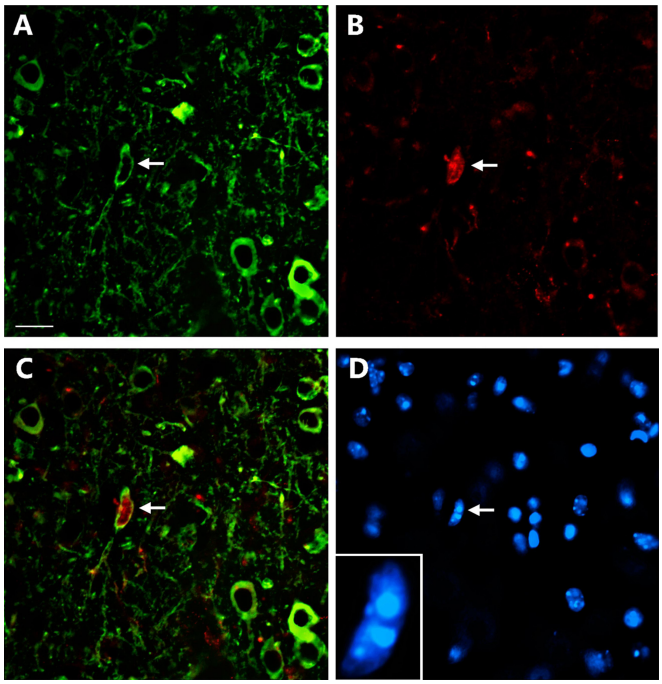

FIGURE 6. A subset of human tau-expressing neurons contains caspase-cleaved substrate and has nuclear morphology indicative of apoptosis. At 2 weeks after delivery of 1.5×10^9 particles of the AAV-tau vector into the lateral entorhinal cortex (EC), a subset of human tau-expressing neurons in layer II of the lateral EC has an abnormal ovoid morphology (**A**, arrow; HT7 staining) and immunostains for caspase substrate cleavage (**B**, arrow; Ab246 staining), visualized by 1-μm digital sectioning. (**C**) Merged figure. (**D**) The same neuron that is positive for caspase activation and has an abnormal shrunken morphology also has chromatin that is condensed and fragmented into apoptotic bodies (arrow; see also the high-magnification inset; Hoechst staining). Scale bars = **(A–D)** 25 μm; inset, 4 μm.

model is distinct from the many transgenic mouse lines that express human tau and develop AD-type tauopathy in the form of tau hyperphosphorylation, aggregation, neurofibrillary tangle formation, and neurodegeneration in a large number of regions of the CNS (50) or focally in the medial perforant pathway (6, 7) and has several favorable experimental features. We provide evidence that mutant human tau induces dose-dependent apoptotic death of the neurons of origin for the lateral perforant pathway and partially deafferents the hippocampus. The mice injected intraentorhinally with the AAV–tau vector mimic aspects of the earliest Braak stage I of Alzheimer tauopathy characterized by tau hyperphosphorylation restricted to the neurons of the superficial entorhinal cortex and their dendritic arbors (4, 41), although they are not engineered to develop tauopathy in other preferential early sites for tau pathology such as the locus coeruleus (59). Furthermore, the model recapitulates the degeneration of perforant pathway neurons and synapses in the elderly that characterizes the transition from normal cognition to early AD-related cognitive impairment (8, 9, 42, 51, 52).

Several lines of evidence indicate that human tauP301L triggers rapid degeneration of mouse perforant pathway neurons in superficial entorhinal cortex. Within 3 weeks, pathologic tau causes the loss of up to 81% of NeuN-positive neuronal nuclei preferentially in layer II of the lateral entorhinal area (Fig. 4). By 12 to 14 days, a large number of acutely degenerating neurons confined to the same entorhinal area label with Fluoro-Jade B, a well-established marker for dying neurons (34); therefore, this represents neuronal degeneration rather than simply marker loss. The toxicity for neurons of the perforant pathway is specific for human tauP301L but not eGFP and is gene dosage dependent. In addition, zinc staining of the afferent lamination in the dentate gyrus and immunolabeling for a presynaptic terminal marker provide evidence that pathologic human tau causes extensive and selective loss of lateral perforant pathway synapses in the OML (Fig. 4; Figure, Supplemental Digital Content 2, http://links.lww.com/NEN/A525). The toxicity of pathologic human tau for the mouse perforant pathway, a circuit preferentially susceptible to tauopathy and

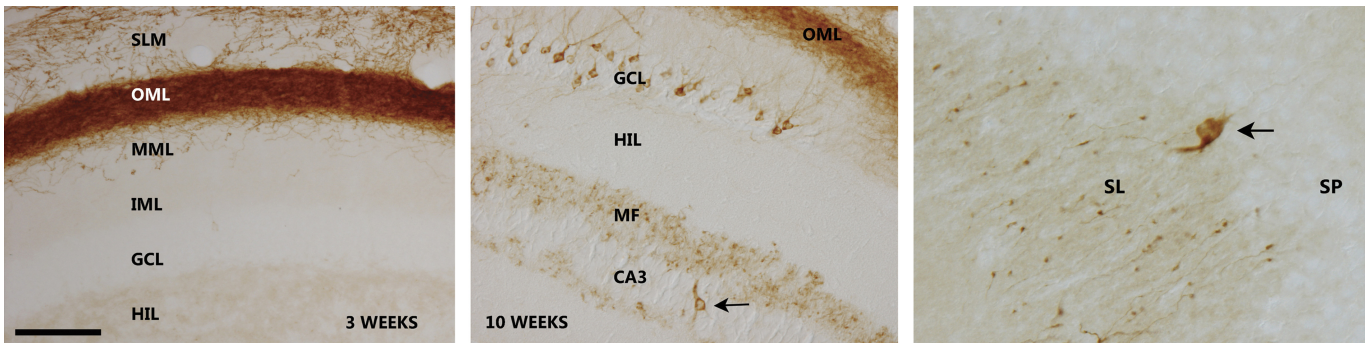

FIGURE 7. Human tau expression expands over time through polysynaptic afferent pathways. (**A**) At 3 weeks after intraentorhinal delivery of 1.5×10^9 particles of the AAV-tau vector, human tau expression in the hippocampal formation detected with HT7 staining is confined to the perforant pathway afferents in the stratum lacunosum-moleculare (SLM) and the lateral perforant pathway synaptic field in the dentate outer molecular layer (OML). (**B**) By 10 weeks, human tau expression expands to include a subset of the granule neuron perforant pathway targets (GCL), the granule neuron mossy fiber projection (MF), and sparse numbers of mossy fiber target neurons in the pyramidal cell layer of the CA3 region (CA3). (**C**) Higher-power view of HT7-positive human tau expression in the mossy fiber axons and boutons in stratum lucidum of the CA3 sector (SL) and the occasional pyramidal cell neuron (SP, arrow) 14 weeks after intraentorhinal delivery of pathologic human tau. Scale bars = **(A)** 120 μm; **(B)** 150 μm; **(C)** 75 μm.

degeneration in the earliest symptomatic stages of AD, further supports the hypothesis that tau plays an important pathogenic role during the progressive neurodegenerative phase of the disease.

The viral vector–based mouse model for early-stage AD tauopathy described here complements recently developed transgenic mouse lines with human tau expression restricted to the medial perforant pathway (6, 7) and has added benefits of speed and flexibility. Our AAV model develops tau hyperphosphorylation, neuronal degeneration, and synapse loss within a few weeks, in contrast to the transgenics with spatially restricted human tau expression, which require 18 months or longer to exhibit perforant pathway damage. The AAV-based tau gene delivery can be unilateral or bilateral, dose titrated, and directed to either the lateral or the medial perforant pathway or potentially to any neural circuit for which the WPRE promotes a strong foreign protein expression. In addition, the AAV vector described here could foster the development of rat and large animal models of AD-type tauopathy with distinct experimental advantages over the mouse.

The rapidity of the AAV model facilitates mechanistic and therapeutic in vivo studies of tauopathy. We exploited this feature to provide evidence that pathologic tau causes apoptotic degeneration of lateral EC layer II neurons. The mutant tau induces nuclear morphologic changes indicative of apoptosis in EC layer II and caspase-mediated substrate degradation in at least a subset of these dying neurons, concomitant with the staining of layer II with Fluoro-Jade B (Fig. 5). Within 2 weeks pi, a subset of lateral EC layer II neurons expressing human tau has an abnormal shrunken morphology, is immunopositive for caspase activation, and exhibits condensation and fragmentation of chromatin. Consequently, although alternative mechanisms for tau neurotoxicity have been described (23–25), our morphologic and immunochemical evidence derived from the perforant pathway, coupled with findings from other in vitro and in vivo systems, suggests that pathologic tau triggers neuronal apoptosis in circuits preferentially vulnerable in AD (19–22).

The tau-driven death of perforant pathway neurons precedes Gallyas-positive neurofibrillary tangles and phosphorylation of the AT100 and PHF1 epitopes that are late markers for tau aggregation (Figure, Supplemental Digital Content 2, http://links.lww.com/NEN/A525) (53), thus adding to evidence that tau neurotoxicity is separable from tangle formation (54–56). The form of tau that triggers apoptotic neurodegeneration and molecular mechanisms by which tau engages the apoptotic machinery are unclear. In this regard, it is notable that, in our model, hyperphosphorylated but not total tau is confined to the entorhinal cortex and is absent from the perforant pathway projection. Further study will be required to assess the contributions of distinct tau phosphoforms, conformers, aggregation states, and alterations in microtubule binding, compartmentalized dephosphorylation, and axonal transport to perforant pathway neurotoxicity.

The development and initial characterization of a rapid gene delivery–based mouse model for early-stage AD-type tauopathy provide a foundation for addressing several unresolved issues. Among them, the factors responsible for the preferential susceptibility of the perforant pathway to tauopathy and degeneration early in the course of AD are unknown. The vulnerability of neuronal populations to tauopathy is not exclusive to the perforant pathway, however, because another type of AAV tau vector can induce rapid toxicity for hippocampal CA1 pyramidal neurons (57) and many regions of the brain and spinal cord are impacted in tau transgenic mice (50). The preferential susceptibility of the perforant pathway to pathologic tau and mechanisms underlying its differential vulnerability are open to further investigation. Another aspect of intraentorhinal tau gene delivery worthy of further study is the polysynaptic expansion of human tau expression over time to hippocampal target neurons (Fig. 7). Although AAV has been used traditionally to drive gene expression locally in the brain, there is evidence from the visual system for anterograde transsynaptic AAV transfer (58). Consequently, at present, it is uncertain whether the human tau or the viral vector spreads polysynaptically in our model. Furthermore, the temporal evolution of tau hyperphosphorylation, aggregation, and neurodegeneration at lower levels of tau expression that are not acutely toxic for the perforant pathway remains to be established. Finally, although the EC is a major source of hippocampal innervation and is critical for at least certain forms of long-term memory, the behavioral functions subserved by the lateral and medial perforant pathways remain to be defined. The technique described here for producing highly circumscribed lesions of the lateral perforant pathway should facilitate dissection of the behavioral functions of this major hippocampal afferent system (59).

ACKNOWLEDGMENTS

We thank Dr. Virginia Lee for generously providing human tauP301L cDNA, Dr. Peter Davies for generously providing the PHF1 antibody, Nicholas Giovannone for assistance with the animals and technical support, and Dr. Arbansjit Sandhu, Shu-Jen Chen, and the rest of the staff of the Penn Vector Core Facility under the direction of Dr. Julie Johnson for preparing the AAV vectors (supported in part by National Institutes of Health grant DK019525 to Dr. Mitchell Lazar).

REFERENCES

1. Amaral D, Lavenex P. Hippocampal neuroanatomy. In: Andersen P, Morris R, Amaral D, Bliss T, O'Keefe J, eds. *The Hippocampus Book*. New York, NY: Oxford University Press; 2007:37–114
2. Squire LR, Wixted JT, Clark RE. Recognition memory and the medial temporal lobe: A new perspective. Nat Rev Neurosci 2007;8:872–83
3. Staubli U, Ivy G, Lynch G. Hippocampal denervation causes rapid forgetting of olfactory information in rats. Proc Natl Acad Sci USA 1984; 81:5885–87
4. Braak H, Braak E. Neuropathological staging of Alzheimer-related changes. Acta Neuropathol 1991;82:239–59
5. Hyman BT, Van Hoesen GW, Kromer LJ, et al. Perforant pathway changes and the memory impairment of Alzheimer's disease. Ann Neurol 1986;20:472–81
6. Liu L, Droulet V, Wu JW, et al. Transsynaptic spread of tau pathology in vivo. PLoS One 2012;7:e31302
7. de Calignon A, Polydoro M, Suarez-Calvet M, et al. Propagation of tau pathology in a model of early Alzheimer's disease. Neuron 2012;73: 685–97
8. Gomez-Isla T, Price JL, McKeel DW Jr, et al. Profound loss of layer II entorhinal cortex neurons occurs in very mild Alzheimer's disease. J Neurosci 1996;16:4491–500
9. Price JL, Ko AI, Wade MJ, et al. Neuron number in the entorhinal cortex and CA1 in preclinical Alzheimer's disease. Arch Neurol 2001; 58:1395–402

10. Hyman BT, Van Hoesen GW, Damasio AR, et al. Alzheimer's disease: Cell-specific pathology isolates the hippocampal formation. Science 1984;225:1168–70
11. Schneider A, Mandelkow E. Tau-based treatment strategies in neurodegenerative diseases. Neurotherapeutics 2008;5:443–57
12. Yoshiyama Y, Lee VM, Trojanowski JQ. Therapeutic strategies for tau mediated neurodegeneration. J Neurol Neurosurg Psychiatry 2013;84:784–95
13. Lewis J, McGowan E, Rockwood J, et al. Neurofibrillary tangles, amotrophy and progressive motor disturbance in mice expressing mutant (P301L) tau protein. Nat Genet 2000;25:402–5
14. Gotz J, Chen F, Barmettler R, et al. Tau filament formation in transgenic mice expressing P301L tau. J Biol Chem 2001;276:529–34
15. Ramsden M, Kotilinek L, Forster C, et al. Age-dependent neurofibrillary tangle formation, neuron loss, and memory impairment in a mouse model of human tauopathy. J Neurosci 2005;25:10637–43
16. Spires TL, Orne JD, SantaCruz K, et al. Region-specific dissociation of neuronal loss and neurofibrillary pathology in a mouse model of tauopathy. Am J Pathol 2006;168:1598–607
17. Berger Z, Roder H, Hanna A, et al. Accumulation of pathological tau species and memory loss in a conditional model of tauopathy. J Neurosci 2007;27:3650–62
18. Yoshiyama Y, Higuchi M, Zhang B, et al. Synapse loss and microglial activation precede tangles in a P301S tauopathy mouse model. Am J Pathol 2007;177:1977–88
19. Chung CW, Song YH, Kim IK, et al. Proapoptotic effects of tau cleavage product generated by caspase-3. Neurobiol Dis 2001;8:162–72
20. Fath T, Eidenmüller J, Brandt R. Tau-mediated cytotoxicity in a pseudohyperphosphorylation model of Alzheimer's disease. J Neurosci 2002;22:9733–41
21. Ramalho RM, Viana RJ, Castro RE, et al. Apoptosis in transgenic mice expressing the P301L mutated form of human tau. Mol Med 2008;14:309–17
22. Messing L, Decker JM, Joseph M, et al. Cascade of tau toxicity in inducible hippocampal brain slices and prevention by aggregation inhibitors. Neurobiol Aging 2013;34:1343–54
23. Allen B, Ingram E, Takao M, et al. Abundant tau filaments and nonapoptotic neurodegeneration in transgenic mice expressing human P301S tau protein. J Neurosci 2002;22:9340–51
24. Liazoghli D, Perreault S, Micheva KD, et al. Fragmentation of the Golgi apparatus induced by the overexpression of wild-type and mutant human tau forms in neurons. Am J Pathol 2005;166:1499–514
25. Spires-Jones TL, deCalignon A, Matsui T, et al. In vivo imaging reveals dissociation between caspase activation and acute neuronal death in tangle-bearing neurons. J Neurosci 2008;28:862–67
26. Ramirez JJ, Poulton WE, Knelson E, et al. Focal expression of mutated tau in entorhinal cortex neurons of rats impairs spatial working memory. Behav Brain Res 2011;216:332–40
27. Carty N, Lee D, Dickey C, et al. Convection-enhanced delivery and systemic mannitol increase gene product distribution of AAV vectors 5, 8, and 9 and increase gene product in the adult mouse brain. J Neurosci Methods 2010;194:144–53
28. Zhang C, McNeil E, Dressler L, et al. Long-lasting impairment in hippocampal neurogenesis associated with amyloid deposition in a knock-in mouse model of familial Alzheimer's disease. Exp Neurol 2007;204:77–87
29. Malthankar-Phatak G, Poplawski S, Toraskar N, et al. Combination therapy prevents amyloid-dependent and -independent structural changes. Neurobiol Aging 2012;33:1273–83
30. Franklin KBJ, Paxinos G. *The Mouse Brain in Stereotaxic Coordinates*, 3rd ed. London, UK: Academic Press, 2008
31. Zhang C, Siman R, Xu YA, et al. Comparison of calpain and caspase activities in the adult rat brain after transient forebrain ischemia. Neurobiol Dis 2002;10:289–305
32. Chen Z, Kontonotas D, Friedmann D, et al. Developmental status of neurons selectively vulnerable to rapidly triggered post-ischemic caspase activation. Neurosci Lett 2005;376:166–70
33. Timm F. Histochemie des Ammonshorn-gebietes. Z Zellforsch 1958;46: 548–53
34. Schmued LC, Hopkins KJ. Fluoro-Jade: Novel fluorochromes for detecting toxicant-induced neuronal degeneration. Toxicol Pathol 2000;28:91–99
35. Gallyas F. Silver staining of Alzheimer's neurofibrillary changes by means of physical development. Acta Morphol Acad Sci Hung 1971;19:1–8
36. Zufferey R, Donello JE, Trono D, et al. Woodchuck hepatitis virus posttranscriptional regulatory element enhances expression of transgenes delivered by retroviral vectors. J Virol 1999;73:2886–92
37. Paterna JC, Moccetti T, Mura A, et al. Influence of promoter and WHV posttranscriptional regulatory element on AAV-mediated transgene expression in the rat brain. Gene Ther 2000;7:1304–11
38. Glover CP, Bienemann AS, Heywood DJ, et al. Adenoviral-mediated, high-level, cell-specific transgene expression: A SYN1-WPRE cassette mediates increased transgene expression with no loss of neuron specificity. Mol Ther 2002;5:509–16
39. Van Groen T, Miettinen P, Kadish I. The entorhinal cortex of the mouse: Organization of the projection to the hippocampal formation. Hippocampus 2003;13:133–49
40. Zheng-Fischhofer Q, Biernat J, Mandelkow EM, et al. Sequential phosphorylation of tau by glycogen synthase kinase-3beta and protein kinase A at Thr212 and Ser214 generates the Alzheimer-specific epitope of antibody AT100 and requires a paired helical filament-like conformation. Eur J Biochem 1998;15:542–54
41. Tolnay M, Mistl C, Ipsen S, et al. Argyrophilic grains of Braak: Occurrence in dendrites of neurons containing hyperphosphorylated tau protein. Neuropathol Appl Neurobiol 1998;24:53–59
42. Kordower JH, Chu Y, Stebbins GT, et al. Loss and atrophy of layer II entorhinal cortex neurons in elderly people with mild cognitive impairment. Ann Neurol 2001;49:202–13
43. Nadler JV, Cotman CW, Paoletti C, et al. Histochemical evidence of altered development of cholinergic fibers in the rat dentate gyrus following lesions. II. Effects of partial entorhinal and simultaneous multiple lesions. J Comp Neurol 1977;171:589–604
44. Vuksic M, Del Turco D, Vlachos A, et al. Unilateral entorhinal denervation leads to long-lasting dendritic alterations of mouse hippocampal granule cells. Exp Neurol 2011;230:176–85
45. Wagner GP, Oertel WH, Wolff JR. Entorhinal lesions result in shrinkage of the outer molecular layer of rat dentate gyrus leading subsequently to an apparent increase of glutamate decarboxylase and cytochrome oxidase activities. Neurosci Lett 1983;39:255–60
46. Geddes JW, Wilson MC, Miller FD, et al. Molecular markers of synaptic plasticity. Adv Exp Med Biol 1990;268:425–32
47. Haug F-MS. Electron microscopical localization of the zinc in hippocampal mossy fibre synapses by a modified sulfide silver procedure. Histochemie 1967;8:355–68
48. Schauwecker PE, McNeill TH. Enhanced but delayed axonal sprouting of the commissural/associational pathway following a combined entorhinal cortex/fimbria fornix lesion. J Comp Neurol 1995;351:453–64
49. Frost B, Jacks RL, Diamond MI. Propagation of tau misfolding from the outside to the inside of a cell. J Biol Chem 2009;284:12845–52
50. Brion JP, Ando K, Heraud C, Leroy K. Modulation of tau pathology in tau transgenic models. Biochem Soc Trans 2010;38:996–1000
51. Thal DR, Holzer M, Rüb U, et al. Alzheimer-related tau pathology in the perforant path target zone and in the hippocampal stratum oriens and radiatum correlates with onset and degree of dementia. Exp Neurol 2000;163:98–110
52. Scheff SW, Price DA, Schmitt FA, et al. Hippocampal synaptic loss in early Alzheimer's disease and very mild cognitive impairment. Neurobiol Aging 2006;27:1372–84
53. Greenberg SG, Davies P, Schein JD, et al. Hydrofluoric acid-treated tau PHF proteins display the same biochemical properties as normal tau. J Biol Chem 1992;267:564–69
54. Andorfer C, Acker CM, Kress Y, et al. Cell-cycle reentry and cell death in transgenic mice expressing nonmutant human tau isoforms. J Neurosci 2005;25:5446–54
55. Brunden KR, Trojanowski JQ, Lee VM-Y. Evidence that non-fibrillar tau causes pathology linked to neurodegeneration and behavioral impairments. J Alzheimer Dis 2008;14:393–99
56. de Calignon A, Fox LM, Pitstick R, et al. Caspase activation precedes and leads to tangles. Nature 2010;464:1201–4
57. Jaworski T, Lechat B, Demedts D, et al. Dendritic degeneration, neurovascular defects, and inflammation precede neuronal loss in a mouse model for tau-mediated neurodegeneration. Am J Pathol 2011;179:2001–15
58. Hennig AK, Levy B, Ogilvie JM, et al. Intravitreal gene therapy reduces lysosomal storage in specific areas of the CNS in mucopolysaccharidosis VII mice. J Neurosci 2003;23:3302–7
59. Attems J, Thal DR, Jellinger KA. The relationship between subcortical tau pathology and Alzheimer's disease. Biochem Soc Trans 2012;40:711–15

